2017 American Control Conference
Sheraton Seattle Hotel
May 24–26, 2017, Seattle, USA

Real-Time Stabilization of Neurons into Clusters

Timothy Matchen
Department of Mechanical Engineering
University of California, Santa Barbara
Email: tmatchen@umail.ucsb.edu

Jeff Moehlis
Department of Mechanical Engineering
University of California, Santa Barbara
Email:moehlis@engineering.ucsb.edu

Abstract— **Deep brain stimulation (DBS) is a widespread method of combating tremors associated with Parkinson's disease, but whose mechanisms are not fully understood. One hypothesis, supported experimentally, is that some symptoms of Parkinson's are associated with pathological synchronization of neurons in the basal ganglia. For this reason, there has been interest in recent years in finding efficient ways to desynchronize neurons that are both fast-acting and low-power. Recent results on coordinated reset and periodically forced oscillators suggest that forming distinct clusters of neurons may prove to be more effective than achieving complete desynchronization by promoting plasticity effects that might persist after stimulation is turned off. Existing proposed methods for achieving clustering frequently require either multiple input sources or precomputing the control signal. We propose here a control strategy for clustering, based on an analysis of the reduced phase model for a set of identical neurons, that allows for real-time, single-input control of a population of neurons with low-amplitude, low total energy signals.**

I. Introduction

Deep brain stimulation (DBS) is a proven method of reducing certain symptoms related to Parkinson's disease (PD), most notably tremors and dyskinesia, wherein an electrode is implanted in either the subthalamic nucleus (STN) or global pallidus internus (GPi) [1], [2]. Despite its proven effectiveness, the mechanisms by which DBS alleviates the symptoms are poorly understood. Additionally, there are risks associated with DBS, both related to the surgical procedure and hardware as well as to the chronic usage in combating the symptoms of PD [1], [3]. For these reasons, there have been various attempts in recent years at not only better understanding the processes that allow for the success of DBS, but also understanding ways to reduce the possible negative side-effects.

Recent work [4]–[8] suggests that symptoms of Parkinson's are associated with elevated synchrony of neurons in the basal ganglia, and there has been experimental and theoretical evidence [9]–[11] that the reduction of this synchrony is correlated to the alleviation of symptoms. One approach to achieve partial desynchronization is to split the neurons into clusters, in which only a subpopulation of the neurons are spike-synchronized. In fact, [10] suggests that the standard DBS protocol leads to clusters.

One promising approach to clustering, coordinated reset, involves using a network of electrode implants delivering a series of identical impulses separated by a time delay between implants. This has been studied extensively [9], [12]–[14] with preliminary clinical success [15]. The method, however, relies on a number of electrodes equal to the number of clusters desired. This may not always be physically feasible in practice. It also requires the powering of multiple electrodes simultaneously, which additionally limits its energy efficiency.

Another approach is to design the control to maximize the desynchronization of the neurons. In [16], this is done using a high-amplitude input to drive neurons close to the unstable fixed point in the interior of the stable limit cycle. [17] develops an optimal control strategy that is more energy-efficient than the "phaseless set" method proposed in [16] but requires more frequent application of the control signal. In both cases, the energy cost represents a substantial improvement over conventional DBS and requires only a single input; total desynchronization, however, may not be preferable, as it returns to a synchronous state more quickly than in clustering (for comparison, see [17] and [14]). Additionally, clustering behavior may contribute to longer-term reduction in pathological synchronization via increased plasticity in the relevant neural regions [18].

[17], [19]–[21] all employ precomputed signals to achieve their control objectives. Like [17], [19] and [20] use optimization principles to derive lowest-energy control strategies for populations of neurons. In [21], heterogeneity in the natural frequencies of the neurons is exploited to entrain clustering of neurons. The use of precomputed, open-loop control signals in these methods reduces their flexibility in real-time application; there is no capacity for adjustment to error in the model. Additionally, the reliance on heterogeneity makes the control scheme highly model-specific, requiring a complete recalculation in the event of alterations to the model or neuron population.

In this paper we develop a control strategy that pro-

978-1-5090-5992-8/$31.00 ©2017 AACC

vides a low-energy, single-input solution with minimal requirement for precomputed information. This strategy can be easily applied to any neuron model to drive the population to a K-cluster state, where K is an arbitrary positive integer as desired for the control objective. The control strategy is designed based on a population of identical neurons subject to a single input; we note that modifications can be made to the strategy to accommodate heterogeneities as well. We will begin in Section II by demonstrating that, provided certain assumptions are made about the neuron population, the population may always be stabilized to a desired control state. With this established, we develop the control strategy in Section III; the strategy is then applied to a neuron population in Section IV.

As in some of the previously cited papers, we will make use of the phase model reduction for the dynamical system in designing our control strategy. The firing neuron oscillates via a fixed, stable limit cycle; following the work in [22]–[24] we can therefore reduce the dynamics when the neuron's state is near the limit cycle to the representation:

$$\dot{\theta_j} = \omega + Z\left(\theta_j\right) u\left(t\right), \tag{1}$$

where $\dot{\theta_j}$ describes the evolution of the jth neuron and the control input, $u\left(t\right)$, is proportional to the applied current I and is common to all neurons. $Z\left(\theta\right)$ is known as the phase response curve, and describes the sensitivity of the phase to a stimulus. The two models in this paper are examples of Type I and Type II neurons [25], respectively. For both models, the phase response curve was calculated by solving the appropriate adjoint equation using the dynamical modeling program XPPAUT [26].

II. General Stabilizability of N Identical Neurons

We demonstrate that any order-preserving clustering scheme for uncoupled, identical neurons is asymptotically stabilizable with an appropriate control input. To do this, it must be shown that the control system is passive with a radially unbounded positive definite storage function and zero-state observable [27]. We will define the storage function, show its passivity, and then show its zero-state observability. We demonstrate this for the case of N identical, uncoupled neurons in the reduced phase model formulation. We label the neurons such that, at time $t = 0$, the neuron phases are ordered as $\theta_1 < \theta_2 < \theta_3 < ... < \theta_N$. Note that if the phases of two neurons are exactly the same, because the neurons are identical and receive identical inputs they are impossible to separate; therefore, we exclude the possibility of two phases being equal by assumption. Furthermore, since the neurons are identical, the response of a neuron is bounded by the neurons of phase initially less than the neuron and those greater than the neuron, so for $t > 0$, it follows from these assumptions that $\theta_1^* < \theta_2^* < ... < \theta_N^*$ (here we do not use the modulo 2π value for θ_j, so θ_j is allowed to be greater than 2π) [20].

Because we are attempting to stabilize to a target trajectory instead of a target state, it is natural to define our storage function in terms of the differences between the phases of neurons rather than the individual phases (which are constantly evolving). More precisely, we construct our storage function as the linear combination of positive semidefinite functions, each prescribing the target separation for the phases of two neurons:

$$v_i = v_i\left(\theta_j - \theta_k\right), \qquad V\left(\theta_1, ..., \theta_N\right) = \sum_{i=1}^{l} \beta_i v_i, \tag{2}$$

with $\beta_i > 0$ and where θ_j and θ_k are the phases of any two neurons whose separation is to be prescribed by the function v_i. The value of l is arbitrary in this context; in Section III, for the specific problem of clustering $l = K$. The individual storage function candidates have three properties:

1) At the target separation $\theta_j - \theta_k = \Delta\theta^*$, $v_i\left(\Delta\theta^*\right) = 0$;
2) For $\theta_j - \theta_k \neq \Delta\theta^*$, $v_i\left(\theta_j - \theta_k\right) > 0$ and grows unbounded away from $\Delta\theta^*$ within the interval $\theta_j - \theta_k \in (0, 2\pi)$;
3) $\left.\frac{\partial v_i}{\partial \Delta\theta}\right|_{\Delta\theta^*} = 0$.

We now calculate the value of $\dot{V}$. As each individual storage function is dependent on only one phase difference, we write $\dot{V}$ as:

$$\dot{V} = \sum_{i=1}^{l} \beta_i \frac{\partial v_i}{\partial \Delta\theta_i} \dot{\Delta\theta_i} = \sum_{i=1}^{l} \beta_i \frac{\partial v_i}{\partial \Delta\theta_i} \left(\dot{\theta_j} - \dot{\theta_k}\right). \tag{3}$$

Substituting in from (1), $\dot{V}$ can be rewritten as:

$$\dot{V} = u \sum_{i=1}^{l} \beta_i \frac{\partial v_i}{\partial \Delta\theta_i} \left(Z\left(\theta_j\right) - Z\left(\theta_k\right)\right). \tag{4}$$

Recalling the definition of passivity [27], the system is passive if the observable is chosen such that $u^T y \geq \dot{V}$. We choose our observable to be a vector $y = \left[y_1, y_2, \cdots, y_l\right]^T$ such that:

$$y_i = \beta_i \frac{\partial v_i}{\partial \Delta\theta_i} \left(Z\left(\theta_j\right) - Z\left(\theta_k\right)\right) \tag{5}$$

Since all neurons receive an identical input, $u^T = \left[u, u, \cdots, u\right]$, it follows that $u^T y \geq \dot{V}$ everywhere in the state-space (as $u^T y = \dot{V}$). Therefore, the system as constructed is not only passive but also lossless. Additionally, y is zero-state observable: at the target state, $\frac{\partial v_i}{\partial \Delta\theta_i} = 0$; $y = 0$ otherwise only if $Z\left(\theta_j\right) - Z\left(\theta_k\right) = 0$, but no such pair of neurons can stay indefinitely in the

set $y = 0$. We can see this by considering:

$$\frac{d}{dt}\left(Z\left(\theta_j\right) - Z\left(\theta_k\right)\right) = \left.\frac{\partial Z}{\partial \theta}\right|_{\theta_j} \dot{\theta_j} - \left.\frac{\partial Z}{\partial \theta}\right|_{\theta_k} \dot{\theta_k}, \quad (6)$$

which, given $\dot{\theta_j} = \dot{\theta_k}$ instantaneously, would require the partial derivative evaluations to be equal for this second derivative to be equal to 0. To remain in the domain where $y = 0$, this would further imply that this equality must hold over the entire period, i.e. $\exists \delta x \in (0, 2\pi) \mid \left.\frac{\partial Z}{\partial \theta}\right|_{x} = \left.\frac{\partial Z}{\partial \theta}\right|_{x+\delta x} \forall x$. Since $\left.\frac{\partial Z}{\partial \theta}\right|_{0} = \left.\frac{\partial Z}{\partial \theta}\right|_{2\pi}$ and $Z\left(0\right) = Z\left(2\pi\right)$, this is true if and only if $Z\left(\theta\right) = const$, which is physically not realized. Therefore, as the system is both passive with an unbounded storage function and zero-state observable, we can conclude that the system can be stabilized by the choice of $u = -\phi\left(y\right)$ where $\phi\left(y\right)$ is locally Lipschitz and $y\phi\left(y\right) > 0$ [27].

III. Control Strategy for K Clusters of Neurons

The goals of developing a control strategy for clustering are threefold:

1) Create a flexible method such that the strategy functions in a way that is agnostic both to the specific neuron model used and the desired number of clusters K;
2) Require as little precomputing as possible so the method is robust to inaccuracies in modeling; and
3) Allow for the control to be easily tuned for parameters of interest, such as maximum input amplitude and speed with which clustering is achieved.

These three conditions can be seen as measures of robustness for the method. A control scheme that meets these three criteria can be altered on the fly by changing only a small number of target parameters, allowing the input to rapidly be tuned to the performance specifications desired. Additionally, deviations from expected results can be compensated for if the input is not constrained to precomputed values, as would be the case with optimal control strategies derived from, for example, variational principles.

The approach proposed here consists of considering the input of maximal instantaneous efficiency (IMIE) rather than precomputed data. Although not necessarily as efficient as true optimization strategies, IMIE requires only knowledge of the phase response curve of the neurons and the current state of the system.

The rest of this section will be structured as follows: first, we will define the two necessary functions for IMIE: a state function and a cost function. Next, we will lay out the details of the control strategy. Lastly, we will see how the reduction of the model for special cases returns results that agree with intuition and past results.

Control of a system of N neurons into K clusters requires the direct control of $2K$ neurons, split into pairs of 2, with each pair of neurons adjacent to each other in phase order. The control is generated in such a way that each pair is driven apart to a target separation of $\frac{2\pi}{K}$ radians. In this way, K clusters are formed by exploiting the boundedness of response described in Section II. For example, if we wished to subdivide a population of 16 identical neurons into 4 clusters and the neurons were ordered by initial phase ($\theta_1 < \theta_2 < ... < \theta_{16}$), the K control pairs would be $\{2, 3\}$, $\{6, 7\}$, $\{10, 11\}$, and $\{14, 15\}$, and the final clusters would be $\{15, 16, 1, 2\}$, $\{3, 4, 5, 6\}$, $\{7, 8, 9, 10\}$, and $\{11, 12, 13, 14\}$. We define a positive semidefinite function $r_{i,j}$ for each control pair; this function is dependent only on the phase difference $\Delta\theta_{i,j} = \theta_j - \theta_i$ and is identically zero at $\Delta\theta_{i,j} = \frac{2\pi}{K}$.

To allow for consistency in the definition of $r_{i,j}$ across choices of K, the value of $\Delta\theta_{i,j}$ is mapped by the function $g\left(\Delta\theta_{i,j}\right)$ such that $g\left(\frac{2\pi}{K}\right) = \pi$. This is done using the piecewise definition:

$$g\left(\Delta\theta_{i,j}\right) = \begin{cases} \frac{K}{2}\Delta\theta_{i,j} & 0 \leq \Delta\theta_{i,j} \leq \frac{2\pi}{K} \\ \frac{(2\pi+1)K-2\pi}{2(K-1)}\left(\Delta\theta_{i,j} - \frac{2\pi}{K}\right) & \frac{2\pi}{K} < \Delta\theta_{i,j} \leq 2\pi \end{cases}. \quad (7)$$

With this mapping, we define the positive-definite function for each pair as follows:

$$r_{i,j} = \begin{cases} \frac{1}{g(\Delta\theta_{i,j})^p} - \frac{1}{\pi^p} & 0 < \Delta\theta_{i,j} \leq \frac{2\pi}{K} \\ \frac{1}{(2\pi - g(\Delta\theta_{i,j}))^p} - \frac{1}{\pi^p} & \frac{2\pi}{K} < \Delta\theta_{i,j} < 2\pi \end{cases}, \quad (8)$$

which is continuous and differentiable everywhere on the domain $(0, 2\pi)$ except at $\Delta\theta_{i,j} = \frac{2\pi}{K}$. p is a parameter whose value can be adjusted to meet control objectives; in the simulations in Section IV, $p = 0.7$. The function can be made first-order differentiable by the replacement of the constant $\frac{1}{\pi^p}$ with a term that is linear in g, though in practice this is not necessary. It does, however, serve as a valid storage function candidate in (2), while maintaining derivatives with the same sign as in (8). Clearly, (8) is greater than zero for all choices of p with $\Delta\theta_{i,j} \neq \frac{2\pi}{K}$ and grows unbounded as $\Delta\theta_{i,j} \to 0$ or 2π.

From here we can define a full-state storage function of the system as:

$$r = \frac{1}{K}\sum_{l=1}^{K} r_{2l-1,2l}. \quad (9)$$

Note that here we have omitted the neurons that are not being directly controlled, and as such our control pairs are relabelled as $\{1,2\}$, $\{2,3\}$,...,$\{2K-1,2K\}$. Since each component of the summation is greater than zero everywhere except at the desired target state, the combined function is also positive-definite and only equal to zero when all pairs of neurons achieve the target separation.

With the state function defined, we turn our attention to the cost function. While any cost function can be used, we select one that penalizes energy usage and the time required to reach the target state. This can be accomplished by defining the cost function:

$$C(t) = \int_0^t \left[u(\tau)^2 + \alpha r(\tau) \right] \mathrm{d}\tau. \tag{10}$$

The value of α can be adjusted to increase or decrease the relative importance of driving the state quickly to its target. The instantaneous cost associated with the state and input at a given time t can be given by taking the derivative and evaluating:

$$\frac{dC}{dt} = u(t)^2 + \alpha r(t). \tag{11}$$

With these two functions defined, the input of maximal instantaneous efficiency can be generated as follows. An optimal path is one that minimizes $C(t)$ as $t \to \infty$. While to truly optimize, the time-dependent input would need to be computed in advance, IMIE aims to produce a near-optimal input by minimizing the cost incurred at each time step instead. We rewrite $C(t)$ in terms of the value of r, which in the uncoupled case monotonically decreases at all times with the appropriate choice of u. Then the total cost as $t \to \infty$ is equal to:

$$\lim_{t\to\infty} C(t) = \int_{r(0)}^{0} \frac{dC}{dr} \mathrm{d}r; \tag{12}$$

by exploiting the chain rule, we equate $\frac{dC}{dr}$ to:

$$\frac{dC}{dr} = \frac{dC/dt}{dr/dt}. \tag{13}$$

In this formulation, the input we choose is designed so that, at all times, the instantaneous magnitude of $\frac{dC}{dr}$ is minimized. This can be interpreted as the input that is most efficient in terms of cost relative to change in r. The value of $\frac{dC}{dt}$ is given by (11). Differentiating r with respect to time yields:

$$\frac{dr}{dt} = \sum_{l=1}^{2K} \frac{\partial r}{\partial \theta_l} \frac{d\theta_l}{dt}. \tag{14}$$

As in (4), we can reorganize this and express it as:

$$\frac{dr}{dt} = u \sum_{l=1}^{K} \frac{\partial r}{\partial \theta_{2l}} \left(Z(\theta_{2l}) - Z(\theta_{2l-1}) \right), \tag{15}$$

which has the characteristic form $-a(\theta_1, ..., \theta_{2K})\, u(t)$. Therefore, $\frac{dC}{dr}$ is equal to:

$$\frac{dC}{dr} = -\frac{u^2 + \alpha r}{au}, \tag{16}$$

where the dependence of a and r on the state $\Gamma = [\theta_1, ..., \theta_{2K}]$ is omitted from the equation for simplicity.

From this, the extrema can be found by differentiating with respect to u; the input used is then set equal to this calculated minimum. Differentiating and rearranging yields:

$$u(t) = \frac{\sqrt{a^2 \alpha r(t)}}{a} = \mathrm{sign}(a) \sqrt{\alpha r(t)}. \tag{17}$$

Note here the positive root is taken because $\frac{dC}{dr}$ is negative (since $\frac{dC}{dt}$ is always positive and $\frac{dr}{dt}$ is negative by construction), and therefore the quantity au must be positive for the entire expression to be negative.

Recalling the definition of $r(t)$, u evolves as a function of the average separation $\bar{\Delta}\theta$ of the control pairs as approximately $\sqrt{\alpha}\bar{\Delta}\theta^{-p/2}$. From this it can be seen that, holding p constant, increasing α corresponds to a $\sqrt{\alpha}$ increase of the maximum amplitude of the input signal. This in turn decreases the response time of the system at the cost, generally, of increasing total power usage and maximum amplitude. In contrast, increasing the value of p while holding maximum amplitude constant (by adjusting α accordingly) will cause a sharper decline in the input signal, reducing power usage but increasing response time. As such, the system can be tuned to meet the desired control specifications– power usage, maximum amplitude, response time– simply by varying α and p accordingly, regardless of the neuronal model being used.

We now turn our attention to the case where $\alpha = 0$ and demonstrate that the method returns a result that is consistent with intuition. With $\alpha = 0$, the original formulation of $\frac{dC}{dr}$ can be simplified greatly, yielding:

$$\frac{dC}{dr} = \frac{-u}{a}. \tag{18}$$

Unlike the case where $\alpha \neq 0$, this is linear and therefore has no minimum; since the only constraint is that $\frac{-u}{a}$ should be positive, a lower-cost control is always achieved by decreasing the magnitude of u. It can be seen that, as predicted by this result, using a bang-bang controller of constant amplitude takes longer (but requires less energy) the smaller an amplitude is used, thereby agreeing that the optimal control from an energy perspective is to use as small an input as possible.

In practice, we do not want the state to be reached in infinite time. If we abstract away from the physical representations of the phase model (which breaks down at high amplitudes of u) and consider only what will allow us to reach the target state in as little time as possible, we would expect that the solution would be to allow the input signal to be as large as possible for all times. We can model this by removing u^2 from the cost function so that $C^*(t) = \alpha r(t)$. Now, $\frac{dC}{dr}$ is given as:

$$\frac{dC}{dr} = \frac{-\alpha r}{au}. \tag{19}$$

As in the case where $\alpha = 0$, this has no minimum, and instead approaches 0 as $u \to \infty$. Therefore, IMIE correctly predicts that for the fastest possible response, u should be allowed to be as large as allowed by the constraints on the system at all times. This trend, as well as the minimal-energy trend, are demonstrated in simulation and shown as solid lines in Fig. 2. While we do not propose IMIE as a fully optimal control strategy, this demonstrates that the method matches basic sanity checks in its application.

IV. Phase Model Results

We conclude by demonstrating that IMIE is both effective in the phase model regime and also an improvement over constant-amplitude control strategies, which require similarly little precomputing. Two neuron models ($N = 50, K = 4$ with clusters of (13,13,12,12)) were tested, the reduced Hodgkin-Huxley model (a type II neuron model) [28], [29] and the thalamic model (a type I neuron model) [30]. Fig. 1 shows the characteristic evolution of both systems as well as the input magnitude. As can be seen, both achieve strong clustering over the course of the simulation, demonstrating that the control scheme is capable of adequately clustering the neuron population. Furthermore, the choice of the distribution of neurons among the clusters was made to be roughly equal, but need not be– to achieve asymmetrical cluster sizes, it is only necessary to change which pairs of neurons are being controlled and similar results can be achieved. Perhaps most importantly, IMIE achieves clustering both quickly and cheaply; Fig. 2 shows a comparison between the response to constant-amplitude control and IMIE. For a given maximum input strength, IMIE is typically both more energy-efficient and faster, and for a given response time, IMIE is always at least as energy-efficient as constant-amplitude control and, for larger amplitudes, significantly more efficient. In particular, IMIE is a dramatic improvement over constant-amplitude control when the objective is to rapidly reach the target state.

V. Conclusion

We have outlined a potentially effective, real-time strategy for controlling neurons via a single electrode using only present-time information. While precomputed strategies may be ultimately more optimal, the control method described can be applied to an arbitrary phase model with no changes to the underlying control scheme, making it ideal for controlling neuron populations without resorting to costly computations and still providing a low-energy solution that could prove effective in reducing the syptoms of PD.

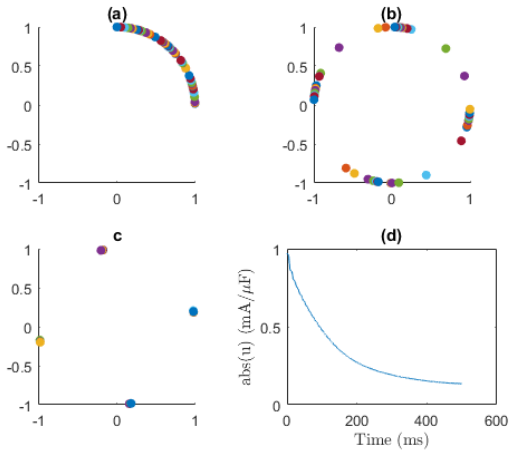

(a)

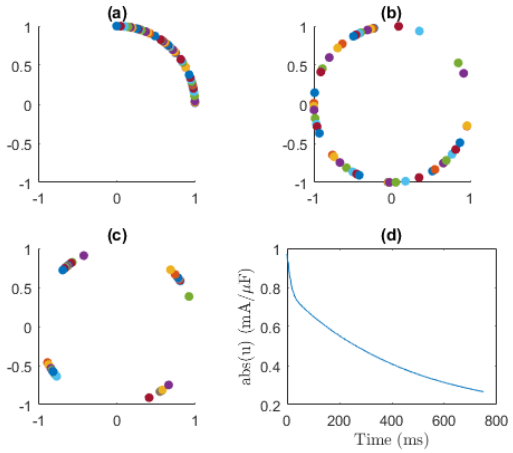

(b)

Fig. 1: Evolution of reduced Hodgkin-Huxley (a) and thalamic (b) phase models at three times. (a), (b), and (c) show the projection of the phases onto the unit circle at times $t = 0$, $t = 125$, and $t = 500$ ms (0, 187.5, and 750 for thalamus), respectively. (d) Shows the absolute value of the input over the length of the simulation. For both models, $\alpha = 0.1$ and $p = .7$.

Acknowledgement

Support for this work by National Science Foundation Grants NSF-1264535 and NSF-1635542 is gratefully acknowledged.

References

[1] M. C. Rodriguez-Oroz, J. A. Obeso, A. E. Lang, J. L. Houeto, P. Pollak, S. Rehncrona, J. Kulisevsky, A. Albanese, J. Volkmann, M. I. Hariz, N. P. Quinn, J. D. Speelman, J. Guridi, I. Zamarbide, A. Gironell, J. Molet, B. Pascual-Sedano, B. Pidoux, A. M. Bonnet, Y. Agid, J. Xie, A. L. Benabid, A. M. Lozano, J. Saint-Cyr, L. Romito, M. F. Contarino, M. Scerrati, V. Fraix, and N. Van Blercom, "Bilateral deep brain stimulation in Parkinson's disease: A multicentre study with 4 years follow-up," *Brain*, vol. 128, no. 10, pp. 2240–2249, 2005.

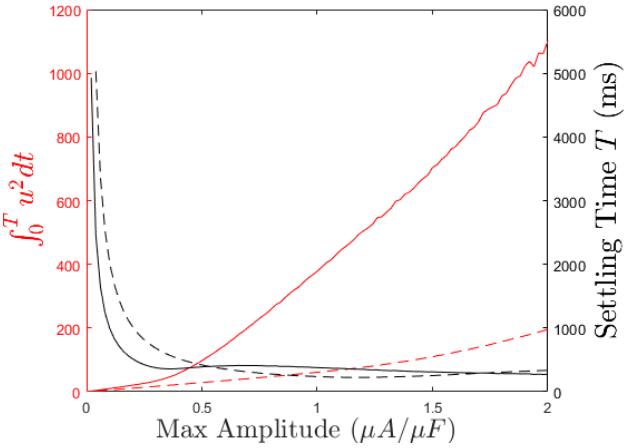

Fig. 2: Comparison of constant-amplitude control (solid lines) and IMIE (dashed lines) for the implementation on the population of uncoupled, identical Hodgkin-Huxley neurons reduced to a phase model for control to the 4-cluster state. The maximum amplitude for each control strategy was varied between $u = 0.02\mu A/\mu F$ to $u = 2.0\mu A/\mu F$. The system was simulated until the value of r reached a target threshold of $r = 0.01$; the value of the settling time T (in black) and cost $\int_0^T u^2 dt$ (in red) are plotted. IMIE outperforms constant-amplitude control over a wide band of control parameters.

[2] The Deep-Brain Stimulation for Parkinson's Disease Study Group, "Deep-brain stimulation of the subthalamic nucleus or the pars interna of the globus pallidus in Parkinson's disease," *New England Journal of Medicine*, vol. 345, no. 13, pp. 956–963, 2001.

[3] A. Beric, P. J. Kelly, A. Rezai, D. Sterio, A. Mogilner, M. Zonenshayn, and B. Kopell, "Complications of deep brain stimulation surgery," *Stereotactic and Functional Neurosurgery*, vol. 77, no. 1-4, pp. 73–78, 2002.

[4] P. J. Uhlhaas and W. Singer, "Neural synchrony in brain disorders: Relevance for cognitive dysfunctions and pathophysiology," *Neuron*, vol. 52, no. 1, pp. 155–168, 2006.

[5] C. C. Chen, V. Litvak, T. Gilbertson, A. Kühn, C. S. Lu, S. T. Lee, C. H. Tsai, S. Tisch, P. Limousin, M. Hariz, and P. Brown, "Excessive synchronization of basal ganglia neurons at 20 Hz slows movement in Parkinson's disease," *Experimental Neurology*, vol. 205, no. 1, pp. 214–221, 2007.

[6] C. Hammond, H. Bergman, and P. Brown, "Pathological synchronization in Parkinson's disease: networks, models and treatments," *Trends in Neurosciences*, vol. 30, no. 7, pp. 357–364, 2007.

[7] R. Levy, W. Hutchison, A. Lozano, and J. Dostrovsky, "High-frequency synchronization of neuronal activity in the subthalamic nucleus of Parkinsonian patients with limb tremor," *The Journal of Neuroscience*, vol. 20, no. 20, pp. 7766–7775, 2000.

[8] A. Schnitzler and J. Gross, "Normal and pathological oscillatory communication in the brain," *Nature Reviews. Neuroscience*, vol. 6, no. 4, pp. 285–96, 2005.

[9] P. A. Tass, "A model of desynchronizing deep brain stimulation with a demand-controlled coordinated reset of neural subpopulations," *Biological Cybernetics*, vol. 89, no. 2, pp. 81–88, 2003.

[10] D. Wilson and J. Moehlis, "Clustered desynchronization from high-frequency deep brain stimulation," *PLoS Computational Biology*, vol. 11, no. 12, pp. 1–26, 2015.

[11] C. J. Wilson, B. Beverlin, and T. Netoff, "Chaotic desynchronization as the therapeutic mechanism of deep brain stimulation," *Frontiers in Systems Neuroscience*, vol. 5, no. June, p. 50, 2011.

[12] L. Lücken, S. Yanchuk, O. V. Popovych, and P. A. Tass, "Desynchronization boost by non-uniform coordinated reset stimulation in ensembles of pulse-coupled neurons," *Frontiers in Computational Neuroscience*, vol. 7, no. May, p. 63, 2013.

[13] B. Lysyansky, O. V. Popovych, and P. A. Tass, "Optimal number of stimulation contacts for coordinated reset neuromodulation," *Frontiers in Neuroengineering*, vol. 6, no. July, p. 5, 2013.

[14] B. Lysyansky, O. V. Popovych, and P. A. Tass, "Desynchronizing anti-resonance effect of m: n ON-OFF coordinated reset stimulation," *Journal of Neural Engineering*, vol. 8, no. 3, p. 036019, 2011.

[15] I. Adamchic, C. Hauptmann, U. B. Barnikol, N. Pawelczyk, O. Popovych, T. T. Barnikol, A. Silchenko, J. Volkmann, G. Deuschl, W. G. Meissner, M. Maarouf, V. Sturm, H. J. Freund, and P. A. Tass, "Coordinated reset neuromodulation for Parkinson's disease: Proof-of-concept study," *Movement Disorders*, vol. 00, no. 00, pp. 1–7, 2014.

[16] P. Danzl, J. Hespanha, and J. Moehlis, "Event-based minimum-time control of oscillatory neuron models: Phase randomization, maximal spike rate increase, and desynchronization," *Biological Cybernetics*, vol. 101, no. 5-6, pp. 387–399, 2009.

[17] D. Wilson and J. Moehlis, "Optimal chaotic desynchronization for neural populations," *SIAM Journal on Applied Dynamical Systems*, vol. 13, no. 1, pp. 276–305, 2014.

[18] C. Zhao, L. Wang, T. Netoff, and L. L. Yuan, "Dendritic mechanisms controlling the threshold and timing requirement of synaptic plasticity," *Hippocampus*, vol. 21, no. 3, pp. 288–297, 2011.

[19] A. Zlotnik and J.-S. Li, "Optimal subharmonic entrainment of weakly forced nonlinear oscillators," *SIAM Journal on Applied Dynamical Systems*, vol. 13, no. 4, pp. 1654–1693, 2014.

[20] J.-S. Li, I. Dasanayake, and J. Ruths, "Control and synchronization of neuron ensembles," *IEEE Transactions on Automatic Control*, vol. 58, no. 8, pp. 1919–1930, 2013.

[21] A. Zlotnik, R. Nagao, I. Z. Kiss, and J.-S. Li, "Phase-selective entrainment of nonlinear oscillator ensembles," *Nature Communications*, vol. 7, pp. 1–7, 2016.

[22] Y. Kuramoto, *Chemical Oscillations, Waves, and Turbulence*, vol. 19 of *Springer Series in Synergetics*. Berlin, Heidelberg: Springer Berlin Heidelberg, 1984.

[23] E. Brown, J. Moehlis, and P. Holmes, "On the phase reduction and response dynamics of neural oscillator populations," *Neural Computation*, vol. 16, no. 4, pp. 673–715, 2004.

[24] P. Sacré and R. Sepulchre, "Sensitivity analysis of oscillator models in the space of phase-response curves: Oscillators as open systems," *IEEE Control Systems*, vol. 34, no. 2, pp. 50–74, 2014.

[25] G. B. Ermentrout and D. H. Terman, *Mathematical Foundations of Neuroscience*, vol. 35 of *Interdisciplinary Applied Mathematics*. New York, NY: Springer New York, 2010.

[26] B. Ermentrout, *Simulating, Analyzing, and Animating Dynamical Systems*. Philadelphia: Society for Industrial and Applied Mathematics, 2002.

[27] H. Khalil, *Nonlinear Control*. New York, NY: Pearson, 1 ed., 2015.

[28] J. Keener and J. Sneyd, *Mathematical Physiology*. Interdisciplinary Applied Mathematics, New York, NY: Springer New York, 2009.

[29] A. Hodgkin and A. Huxley, "A Quantitative Description of Membrane Current and Its Application to Conduction and Excitation in Nerve," *Journal of Physiology*, no. 117, pp. 500–544, 1952.

[30] J. E. Rubin and D. Terman, "High frequency stimulation of the subthalamic nucleus eliminates pathological thalamic rhythmicity in a computational model," *Journal of Computational Neuroscience*, vol. 16, no. 3, pp. 211–235, 2004.